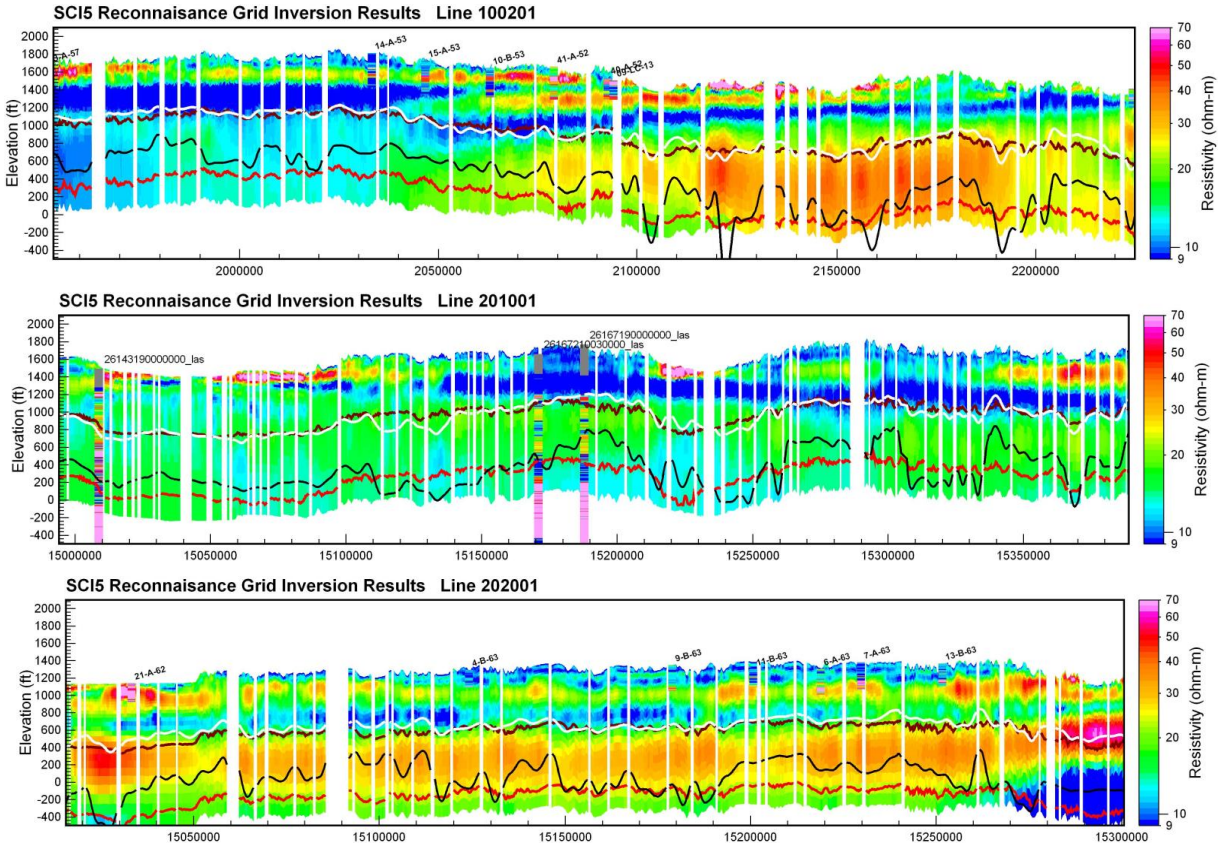
APPENDIX 3 – Depth of Investigation

A Discussion on Depth of Investigation in Geophysics and AEM Inversion Results

Ted Asch, Trevor Irons, Jared Abraham

XRI Geophysics



EXPLORATION RESOURCES INTERNATIONAL

EXECUTIVE SUMMARY

Exploration geophysics, in its most basic form, is the application of the principles of physics to studying physical properties of the earth. But just being able to measure data related to the physical properties of the subsurface is not enough. Usually someone is most interested in certain properties, and usually changes in properties, down to, or specifically at, a certain depth which is going to be, for that particular project, the "depth of interest". Then, because the earth down to the depth of interest must be characterized, sampling protocols requires that the depths investigated must be well below the depth of interest. Therefore geophysical surveys must be designed appropriately to meet all these requirements.

This leads to estimating the "Depth of Investigation" (DOI) in an investigation. The DOI usually refers to the depth below which acquired surface (or airborne) data are insensitive to the physical properties of the earth. That is, at what depth(s) have/do the geophysical techniques used in an investigation become insensitive to variations in the subsurface?

Note that there is a difference between *resolution* of a property and *detection* of a property. Resolution means that the properties of interest are accurately determined. Detection relates the fact that while the true value of a property may not be accurately recovered through inversion, there is still some sensitivity, in the data, to changes in that property and that is what is observed. Furthermore, solutions to electromagnetic induction data are non-unique and understanding how a particular recovered model fits into the distribution of equivalent models is an additional component of model appraisal. Most authors treat the DOI as a line of demarcation between resolution and detection.

In their paper Christiansen and Auken (2012) sum up the value of the DOI as follows: "*A calculation of the DOI is crucial when building geologic or hydrological models from EM data as the validity of the models varies strongly with data noise and the resistivity of the layers themselves. Without the DOI estimate, it is next to impossible to judge when the information in the model is driven by the data or is just an effect of the starting model or the regularization of the inversion.*"

This paper first presents the theoretical basis for estimation of the DOI per Nabighian and Macnae (1989) using electromagnetic skin-depth calculations based on averaged resistivities of a section. Next, a practical determination of DOIs using data-to-model sensitivities inherent to the Jacobian matrix (Christiansen and Auken, 2012) is presented. Finally, a methodology by Oldenburg and Li (1999) based on first inverting

multiple reference models with very different starting halfspace resistivities and, then, comparing the results to determine what are data-driven and what are model-driven.

Examples of AEM data acquired by XRI in Nebraska in October 2014 are presented as a means of demonstrating the process by which AEM DOI's are developed. First Aarhus Workbench Spatially-Constrained Inversion (SCI) results are presented along with the DOIs that the program calculates by default (using cumulative sensitivity thresholds of 1.2 and 0.6). Since there are well-defined geologic features apparent beneath the default DOIs, these inverted earth models suggest that the actual depths of investigation, i.e. resolution/detection, at least for the geologic conditions presented here, are much deeper than what the default DOIs would indicate.

Alternative measures of DOIs based on the same cumulative sensitivity dataset are developed and compared to the default DOI's. DOI's for cumulative sensitivity thresholds 0.1, 0.2, and 0.4 are presented and compared to the DOI's based on thresholds 1.2 and 0.6. The comparison of the new DOI's with the observed features in the SCI inversion results indicates that the DOI based on a global cumulative sensitivity threshold of 0.1 would seem to be a more appropriate DOI on which to base an interpretation.

For comparison's sake, analytical/theoretical DOI's were calculated based on different data noise levels. The DOI for a "typical" maximum winter TEM noise level of 0.5 nV/m^2 is several hundreds of feet deeper than the 0.1 cumulative sensitivity DOI. This is expected, as this approach is concerned with impact of the model on the data, and not necessarily the recoverability of the model. Two more analytical DOI's using noise levels of 4 nV/m^2 and 150 nV/m^2 were developed and these overly the 0.1 and 0.6 cumulative sensitivity DOI's quite well. Spies (1989) states that the summer TEM noise levels are in the range of 2 nV/m^2 to 10 nV/m^2. Since the example data were acquired in October, a noise level of 4 nV/m^2 is reasonable supporting the case that the 0.1 cumulative sensitivity DOI is reasonable. A noise level of 150 nV/m^2, which overlies the 0.6 DOI, is considered to be too high to be reasonable for the presented data.

Ground-truth comparison is accomplished via nearby borehole resistivity logs. Borehole data were used as *a priori* constraint information in the inversion if the boreholes were within 3280 ft (1000 m) of a flight line. While some of the shallow boreholes presented in this DOI analysis were within this distance, they did not have a major effect on the models at the depths of investigation.

For the presented data set, Nebraska CSD and NGOC logs were overlain, for comparison, on the AEM inversion profiles. The shallow, near-surface resistivity zones in the AEM profiles match up well, as expected, with the CSD borehole logs. The

deeper NGOC logs, which were not used as constraints in the inversion, also match up very well with the deeper resistivity zones indicated in the AEM data even though the boreholes are offset from the flight lines by 10,000 ft to 40,000 ft.

Additional validation is accomplished via application of the methodology presented by Oldenburg and Li (1999). SCI inversion results using reference models with halfspace resistivities of 40 ohm-m and 3 ohm-m were compared to the "best fit" results that used a starting halfspace resistivity of 10 ohm-m. The 3 ohm-m starting halfspace inversion results did not converge down to the same error levels as the 10 ohm-m and the 40 ohm-m inversion runs and so could not be used for comparison purposes. However, the 10 ohm-m and the 40 ohm-m inversion runs did have similar measures of error misfits and the results compared very well down to a depth in the vicinity of the DOI based on the 0.1 cumulative sensitivity threshold. Thus, for the non-linear inversion used here, the starting model can affect which local minimum the inversion converges too. This is, effectively, a limited model space investigation of equivalence.

To quantify the comparison, "DOI Index" values were calculated per Oldenburg and Li (1999), and displayed along with the SCI inversion results for the two different starting halfspace models. The 0.2 to 0.4 DOI Index range that Oldenburg and Li suggest might be the separation between inversion results that are data driven and those that are model objective function driven agrees quite well with the DOI based on the global cumulative sensitivity threshold 0.1. The 0.6 DOI lies well within the DOI Index zone where the models match very well. That is, there are several hundred feet of data below the 0.6 DOI which, per the Oldenburg-Li DOI Index methodology, still presents credible interpretation information.

Summarizing, the inversion results from multiple AEM data sets that have been processed and inverted through the Aarhus Workbench suggest that the DOI's exported with the Workbench inversion results, are too conservative and dismiss valuable subsurface information. Additional DOIs have been developed from other cumulative sensitivity thresholds including 0.4, 0.2, and 0.1. Plotting these DOIs on top of inversion results profiles allows for discrimination of the data-driven results and the inversion regularization results. It is clear that, while variable, the global cumulative sensitivity threshold that should be used to determine appropriate DOI's for interpretation of AEM data is much closer to 0.1 than it is to 0.6.

Finally, one must keep in mind the earlier discussion of a depth of resolution where the properties are well recovered and a depth of detection where contrasts are indicated but accurate values are not determined. The DOI that is selected is a somewhat arbitrary choice depending on what it is that the DOI is supposed to represent. In the

case of the AEM data discussed here, the 0.1 DOI represents a depth range separating well resolved information from a range of detected contrasts. This suggests that it is worth retaining as much of the sensitivity information we have, regardless of whether or not those parts of the model are completely well determined.

Table of Contents

1.0 Introduction 9
2.0 Basic Theoretical Background on DOI's 10
3.0 AEM Data Analysis and Inversion 13
4.0 Determination of the DOI 14
4.1 Christiansen-Auken DOI 14
4.2 Oldenburg-Li DOI 17
4.3 Model Space Analysis 19
5.0 AEM Data Example 19
5.1 The GERDA Database 19
5.2 SCI Inversion Results 20
5.3 DOI Contours – Original Set 22
5.4 Comparison of the Theoretical DOI to the Workbench DOI's 24
5.5 DOI Contours – Expanded Set 24
5.6 Ground Truth - DOI Contours and Boreholes 29
5.7 Oldenburg-Li Method For Determination of the DOI 34
6. Discussion and Conclusions 38
7. References 40

List of Figures

1. Illustration of the inverse relationship between changes in resistivity (the inverse of the conductivity s) and theoretical depth of investigation……..4
2. Example sensitivity plots from Christiansen-Auken (2012)…… 8
3. Example of Oldenburg-Li (1999) process for determining the DOI…….. 10
4. Example of exported sensitivities from the GERDA database and the calculated cumulative sensitivities…….. 13
5. Aarhus Workbench SCI inversion results with the "upper" and "lower" DOI's……. 15
6. Aarhus Workbench SCI inversion results with the "default" upper and lower DOI's plus the theoretical DOI using a 0.5 nV/m^2 noise level…… 17

7. Example of exported sensitivities from the GERDA database and calculated cumulative sensitivities for global thresholds 1.2, 0.6, 0.4, 0.2, and 0.1……..…. 19

8. Aarhus Workbench SCI inversion results with DOI's based on cumulative sensitivity global thresholds 1.2, 0.6, 0.4, 0.2, and 0.1…….. 20

9. Aarhus Workbench SCI inversion results with DOI's based on cumulative sensitivity global thresholds 0.6 and 0.1 and available borehole resistivity logs…….. 23

10. SCI inversion results with DOI's based on cumulative sensitivity thresholds 0.6 and 0.1, borehole resistivity logs, and theoretical DOIs based on equation (4) using 4.0 nV/m^2 and 150 nV/m^2 noise levels……. 24

11. SCI inversion results with DOI's based on cumulative sensitivity thresholds 0.6 and 0.1 (black line) and available borehole resistivity logs for three different starting halfspace models – 40 ohm-m, 10 ohm-m, and 3 ohm-m……..…. 26

12. SCI inversion results with cumulative sensitivity DOI's and the associated Oldenburg-Li DOI Index plot. Top: 40 ohm-m starting halfspace. Middle: 10 ohm-m starting halfspace. Bottom: Calculated Oldenburg-Li DOI Index……..…… 28

1.0 Introduction

Exploration geophysics, in its most basic form, is the application of the principles of physics to studying physical properties of the earth. But just being able to characterize physical properties of the subsurface is not enough. Usually someone is most interested in certain properties, and usually changes in properties, down to, or specifically at, a certain depth which is going to be, for that particular project, the "depth of interest". Since the earth down to the expected depth of resolution must be well characterized (i.e. develop a representation of the subsurface to the best ability of the geophysical technique applied), then sampling protocols require that the depths investigated must be well below the depth of resolution. Therefore geophysical surveys must be designed appropriately to meet these requirements.

This leads to estimating the "Depth of Investigation" (or DOI). DOI estimation plays a critical role in survey design as well as data interpretation. The DOI usually refers to the depth below which acquired surface (or airborne) data are insensitive to the nature of the physical properties of the earth. That is, at what depth(s) have/do the geophysical techniques used in an investigation become insensitive to variations in the subsurface? And then how, when examining a model of the earth produced by numerical inversion that has met certain minimized model error criteria, does one determine the DOI? The fact that the DOI is intrinsically linked to the method of model recovery (numerical inversion) means that determining this value is not intuitively obvious. Oldenburg and Li (1999) phrase these questions of model appraisal as: *Which features in the recovered model emulate those in the true earth? What confidence does one have in the existence of the features? And are there artifacts at depth, which if interpreted, would lead to misleading interpretations?* These are issues that must be considered when assigning DOI's to models of inverted data.

Plus, as one can well imagine, different exploration techniques (measuring different physical properties) have very different DOI's depending on the physics of the technique utilized and on the geologic environment in which it is applied in addition to ambient, or inherent, noise levels.

Note that there is a difference between *resolution* of a property and *detection* of a property. Resolution means that the properties of interest are accurately recovered through inversion. Detection relates the fact that while the true value of a property may not be accurately resolved, there is still some sensitivity of the data to changes in that property. For example, it may be clear that the model is changing at depth, even though the true value cannot be determined. Most authors treat the DOI as a line of demarcation between resolution and detection. The appropriateness of this definition,

or whether it can be relaxed to include zones where change in parameters are being detected, though not resolved, is dependent upon survey goals and application.

Thus, over the years, many processes have been published in geophysical research journals for estimating depths of investigation for different exploration techniques and how one goes about determining what DOI should be expected and/or observed when using a particular tool or working in a particular environment.

Several of these are now discussed with particular emphasis on determining an appropriate DOI when conducting an airborne electromagnetic (AEM) investigation using the SkyTEM Time-Domain EM (TDEM) platform. We begin with a theoretical basis for depth of penetration in the earth followed by an application to XRI-acquired SkyTEM data.

2.0 Basic Theoretical Background on DOI's

To understand which parameters affect the depth of penetration of electromagnetic energy, it is helpful to consider the diffusion and attenuation of EM fields within the earth. A theoretical discussion on DOI's for different geophysical tools, configurations, and geological conditions was presented by Nabighian and Macnae (1989) with a follow-up by Spies (1989). For a frequency-domain electromagnetic (FDEM) system, Nabighian and Macnae show that the 'skin' depth at which the electromagnetic field is reduced to 1/*e,* or 37 percent of its value at the surface, is

$$\delta = \sqrt{\frac{2\rho}{\mu_0 \omega}} \qquad (1)$$

where δ is the "skin" depth of penetration in meters, ρ is the electrical resistivity (equals $1/\sigma$), μ_0 is the magnetic permeability in a vacuum, and $\omega = 2\pi f$ is the angular frequency with f being the source frequency in Hz. This equation, appropriate for a uniform earth with one-dimensional (1-D) plane wave incident fields, implies that for a fixed resistivity, as the frequency increases, the depth of exploration decreases. Also note that the skin depth represents an arbitrary cutoff of the diffusive propagation of the field.

Similarly, in the time domain, the depth of the maximum transient electric field (the time-domain diffusion depth) is given by

$$\delta = \sqrt{\frac{2\rho t}{\mu_0}} \qquad (2)$$

where t is time in seconds. It is clear from this equation that, for a fixed resistivity, as time increases (i.e. at later times along the decay curve), the depth of penetration also increases.

For a time-domain near-zone sounding, in which case the loop size or source-receiver separation is less than the depth of investigation which is the case for AEM systems, the DOI is

$$DOI = 0.55\left(\frac{IA}{\sigma V}\right)^{\frac{1}{5}} \tag{3}$$

where I is current and A is the area of the transmitter loop.

If the response voltage V is equated to the base noise level n_V (where we lose sensitivity, i.e. the DOI), then equation (3) becomes

$$DOI = 0.55\left(\frac{IA}{\sigma \eta_V}\right)^{\frac{1}{5}} . \tag{4}$$

For an AEM noise level n_V of 0.5 nV/m^2, then the DOI becomes

$$DOI = 40\left(\frac{IA}{\sigma}\right)^{\frac{1}{5}} . \tag{5}$$

Depths of penetration in a multi-layered earth can be estimated by replacing ρ in the above equations with an 'effective' or averaged resistivity of the ground overlying the desired depth of investigation.

Spies (1989) presented a multi-layered earth model study illustrating the effect of changes in depth of penetration with changes in resistivity. The illustration (Figure 1) shows that as the electrical conductivity increases, the depth of penetration/investigation decreases.

Spies (1989) points out that the practical limitation on the depth of investigation for TDEM systems is a function of the system transmitting power (known as the 'moment' of the system), the time after turn-off at which the signal levels have decayed to ambient background noise levels, and, as shown in Figure 1, the resistivity/conductivity of the earth. Thus, the theoretical/analytical definition of the DOI is the thickness of overburden at which the received signal matches the noise level.

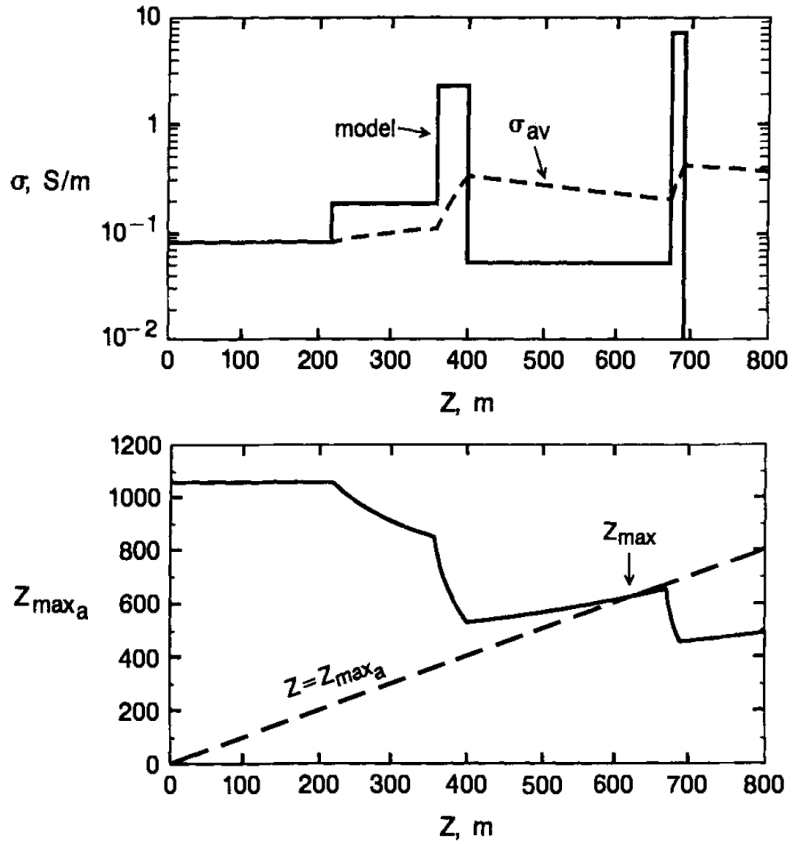


Figure 1. Illustration of the inverse relationship between changes in resistivity (the inverse of the conductivity s) and theoretical depth of investigation (from Spies, 1989). As the electrical conductivity increases (resistivity decreases) in the top figure, the depth of investigation decreases (bottom figure).

Since Nabighian-Macnae (1989) and Spies (1989) were published, geophysical data acquisition, processing, inversion, and interpretation have progressed quite far from theoretical approximations using 'effective'/average resistivities. Advances in electronic and computational hardware including moving from 16 bit to 24 bit to 32 bit data acquisition systems and advances in computation power have allowed development of additional approaches as to how geophysical depths of investigation can be estimated/determined. Instead of approaching an estimation of the DOI just from the theory of the acquisition system (i.e. only the potential data space), DOI's can now also be deduced in the inverted model space in combination with the data space. That is, one examines the numerical inversion results presented as an earth model and investigates the numerical resolution displayed and the observed sensitivities of the model to the acquired data. It is now standard practice for the inversion programs presently in use to produce and report estimated DOI's. However, it should be stressed that there are numerous ways to approach this problem. And due to the need for some type of cutoff of a slowly varying loss of resolution, demarcating one true DOI value is

not a meaningful concept. Instead, the idea of a DOI must be taken into account given the interpretation goals.

3.0 AEM Data Analysis and Inversion

In 2014 XRI Geophysics acquired nearly ten thousand line-kilometers of airborne TDEM data with various SkyTEM systems including the 301, the 304, and the 508 platforms at different locations in the United States (eg. Carney et al., 2014). The AEM data collected by the SkyTEM systems are processed using Aarhus Workbench (Aarhus, 2013), Geosoft Oasis Montaj (Geosoft, 2014), and Profile Analyst (Pitney Bowe, 2012).

The AEM data are first submitted to automatic processing algorithms included in the Aarhus Workbench program including filtering GPS locations, tilt meter, and altimeter readings. Then the TDEM data are manually examined for possible electromagnetic coupling with surface and subsurface power lines and buried metal pipes as well as for late time noise levels. Compromised data are masked out from the inversion. The residual magnetic field data, which is also usually acquired as a matter of standard practice, as well as 60 Hz power line data are also used to examine and, if necessary, remove coupling effects. In addition, the results of the automatic filtering processes are examined. In some instances, AEM data that had been removed by the automatic filters are unmasked in the event that the automated processes identified false-positive matches for coupling. This last, critical, step of quality control is overseen manually.

The TEM data are then inverted using a laterally-constrained inversion (LCI) algorithm in which neighboring soundings along a single flight line are used to constrain the inversion of each sounding. The number of soundings acting as the lateral constraints are an inversion parameter that is expressed as a distance along the line of data on either side of the sounding being inverted. We usually adopt a starting halfspace model consisting of 30 layers, each with a starting resistivity representative of the units at depth for the local geology. The models are usually set to a maximum depth based on the acquisition system moment with the thickness of the layers increasing with depth. The vertical resistivity standard deviation is usually set to 2, while the lateral resistivity standard deviation is set to 1.6.

Following the LCI, profile and depth slices are created to examine the results of the inversion. In the event that remaining electromagnetic couplings are located in the sections, the data are again manually edited and additional LCI's are performed.

Once the results of the final LCI are determined to be free of electromagnetic couplings, a spatially-constrained inversion (SCI) is performed. "Spatial" constraints

refer to using soundings both along the same flight line as the sounding being inverted and on neighboring AEM lines, within a certain distance set by the user. Similarly, the starting model consists of 30 layers, each with the same starting resistivity as the LCI's. For all inversion runs, the maximum depth is based on the moment of the acquisition system and the thickness of the model layers increase with depth by a factor of 1.07.

Once again, the inversion results are examined via profiles and depth slices. If any remaining electromagnetic coupling are detected, they are edited out and the inversions run again. When the inversion results are of sufficient quality and exhibit appropriate data misfit, the resulting models are then exported from the Aarhus Workbench as ASCII XYZ data files and reformatted for display in Encom's visualization software Profile Analyst (Pitney Bowe, 2012).

4.0 Determination of the DOI

In addition to inverting the AEM data, Aarhus Workbench also calculates depths of investigation (DOI) for each inverted sounding. In this section we take a detailed look at the approach used by the developers of the Aarhus Workbench and another approach presented by Oldenburg and Li (1999) to estimate practical DOIs.

As discussed above, the DOI is a numerical estimation of the depth below which the resolution of a model, resulting from a numerical inversion, diminishes. This depth develops primarily due to the limitations of the TDEM method including: the equipment and methodology used for data acquisition, the noise in the data, and the resistivity structure (i.e. the geology) being investigated (Christiansen and Auken, 2012). The result is decreased confidence in observable features in the earth model below the DOI.

4.1 Christiansen-Auken DOI

The ASCII xyz file exported from the Aarhus Workbench after an SCI inversion includes, along with all the inversion model and error data, two columns labeled "DOI_Upper" and "DOI_Lower". 'Upper' refers to a shallower DOI and 'Lower' refers to a deeper DOI. The derivation of these depths, summarized in the next few paragraphs, is presented in Christiansen and Auken (2012).

Unlike the theoretical estimations of the DOI presented in Spies (1989), Christiansen and Auken (2012) developed the Aarhus Workbench so that it uses model sensitivities (the Jacobian) determined during the last inversion step, along with an estimate of data uncertainty to calculate the DOI's. The Jacobian matrix is the sensitivity of the data to perturbations at the current location in model-space. As such, the Jacobian is also a

representation of the sensitivity of changes in the model to the observed data. Mathematically, a sensitivity matrix, G, the Jacobian, can be represented as

$$G_{ij} = \frac{\partial \log(d_i)}{\partial \log(m_j)} \quad , \tag{6}$$

where G_{ij}represents the sensitivity to the i th data point d_i from the j th model parameter m_j.

The next step in the Aarhus DOI calculation is to sum each column of G and normalize by the standard deviation of the data points, Δd_i. The result is an error normalized sensitivity s of each of the model parameters j in the model as calculated by

$$s_j = \sum_{i=1}^{N} \frac{G_{ij}}{\Delta d_i} \quad , \tag{7}$$

where N is the number of observed data points in d. The vector s represents the total error normalized sensitivities for the model parameters with respect to all the data.

The next step according to Christiansen and Auken (2012) is to normalize the error-normalized sensitivities, s_j, by the thickness, t_j, of each layer,

$$s_j^* = \frac{\sum_{i=1}^{N} \frac{G_{ij}}{\Delta d_i}}{t_j} \quad . \tag{8}$$

The last step is to calculate the cumulative sensitivities, S, by summing up the individual thickness-normalized sensitivities starting with the bottom layer. That is, for a 30-layer model (which is usually used in all the XRI Workbench inversions) the cumulative sensitivity for the 30th layer is the thickness-normalized sensitivity for the 30th layer. Then the cumulative sensitivity for the 29th layer is the sum of the cumulative sensitivity for the 30th and the thickness-normalized sensitivity for the 29th layer. The cumulative sensitivity for the 28th layer would be the sum of the cumulative sensitivity for the 29th layer and the thickness-normalized sensitivity for the 28th layer. And so on up to model layer 1. Mathematically speaking, this is given by

$$S_j = \sum_{i=M,-1}^{j} s_i^* \quad . \tag{9}$$

The elements of S_j represent the cumulative sensitivities for a given sounding. That is, S represents the sensitivity to the model that was reached during the inversion. It is from an interpolation of the elements of S_j that the DOI values at set "global" thresholds are selected. "Global" is the term used by Christiansen and Auken (2012). Note that the formulation used by Christiansen and Auken (2012) does not incorporate sensitivity to nearby equivalent models. In other words, the ability of the inversion to distinguish electrically equivalent models from the produced result.

Figure 2 presents example sensitivity plots included in Christiansen and Auken (2012).

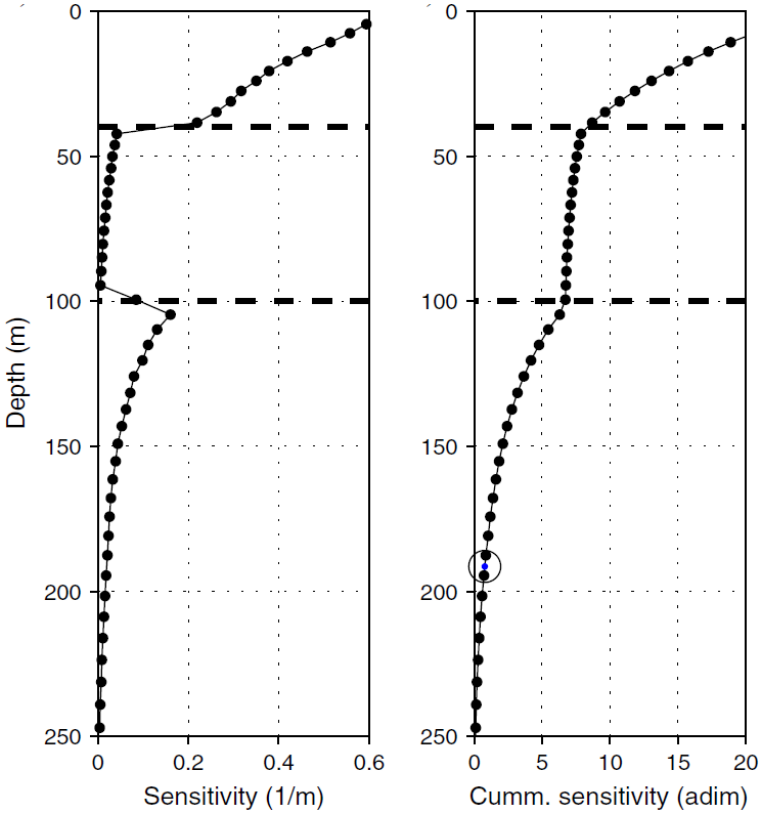


Figure 2. Example sensitivity plots from Christiansen-Auken (2012). Left - Error-, thickness-normalized sensitivity; Right - Cumulative sensitivity plot. The circle indicates the DOI given by a threshold value of 0.8.

As indicated in the caption of Figure 2, a cumulative senstivity threshold value of 0.8 was used by Christiansen and Auken (2012) to select the DOI for that sample sounding. They define the threshold value selected as that cumulative sensitivity which indicates "*the miminum amount of sensitivity needed for indicative information*". Christiansen and Auken (2012) further state that "*setting the threshold value is very much a question of fine-tuning based on experience, intuition, and comparing different models with different methods. The threshold value suggested here is purely*

empiric…. Setting a higher threshold value will decrease the DOI, and a lower value will increase the DOI. In the experimental fine-tuning we have considered values in the range from 0.6 to 1.2." The upper and lower DOIs exported by the Aarhus Workbench are for cumulative sensitivities 1.2 (upper DOI) and 0.6 (lower DOI).

Also, "*We have here consistently shown the DOI as a single number, even though this is somewhat contradicting to the diffusive nature of EM and DC methods, suggesting that information gradually fades away with depth. …… We have tried to present DOI with an upper and a lower value as well, but that has not been well received. Geophysicists wanting to take full advantage of the DOI computations could easily use the full sensitivity kernels….*" Later, in section 5.5, we examine the use of additional elements of the cumulative sensitivity matrix as a means of determining more appropriate DOIs.

4.2 Oldenburg-Li DOI

The Oldenburg and Li (1999) approach involves performing separate inversions with different objective functions (i.e. halfspace reference model resistivities) with the difference between the resulting inverted models being used to determine if the resultant earth model is data-driven or is driven by the regularization of the inversion. Visual examination of plots of the inversion results and calculation of a quantitative measure of the match between models (called the "DOI Index") can provide locations where large differences occur indicating that the model features are no longer controlled by the data.

The advantage of this approach is that it ensures that the full system transfer function is used in each inversion run. However, this approach also requires that the inversion be performed at least two additional times at much different reference model resistivities from the original halfspace reference model resistivity. Note that setting different constraints, because of the diverse resistivity ranges, can have a strong effect on the inversion results. One would think that this would be standard practice (to keep the same constraints for the different inversion runs), but, depending on the specific numerical mechanics of the inversion when dealing with results very far away from the most optimum model, different initial constraints may have to be utilized in order to let the inversion process be successful to some degree. Oldenburg and Li (1999) state it this way: "Usable information comes only when additional constraints such as those required by the model objective function are imposed upon the models". However, to make comparisons, the degree of fit between the different inversions must be similar. Otherwise, comparisons made will not be fully valid.

An example of the Oldenburg-Li (1999) process is illustrated by a figure from their paper (Figure 3). In this case, the optimum model was obtained using a halfspace reference model of 400 ohm-m (Figure 3b). Then Oldenburg-Li run two additional models with reference model halfspaces of 4000 ohm-m (Figure 3a) and 40 ohm-m (Figure 3c). The resulting models can then be analyzed in order to determine the depth at which the solution is being driven by the model objective function.

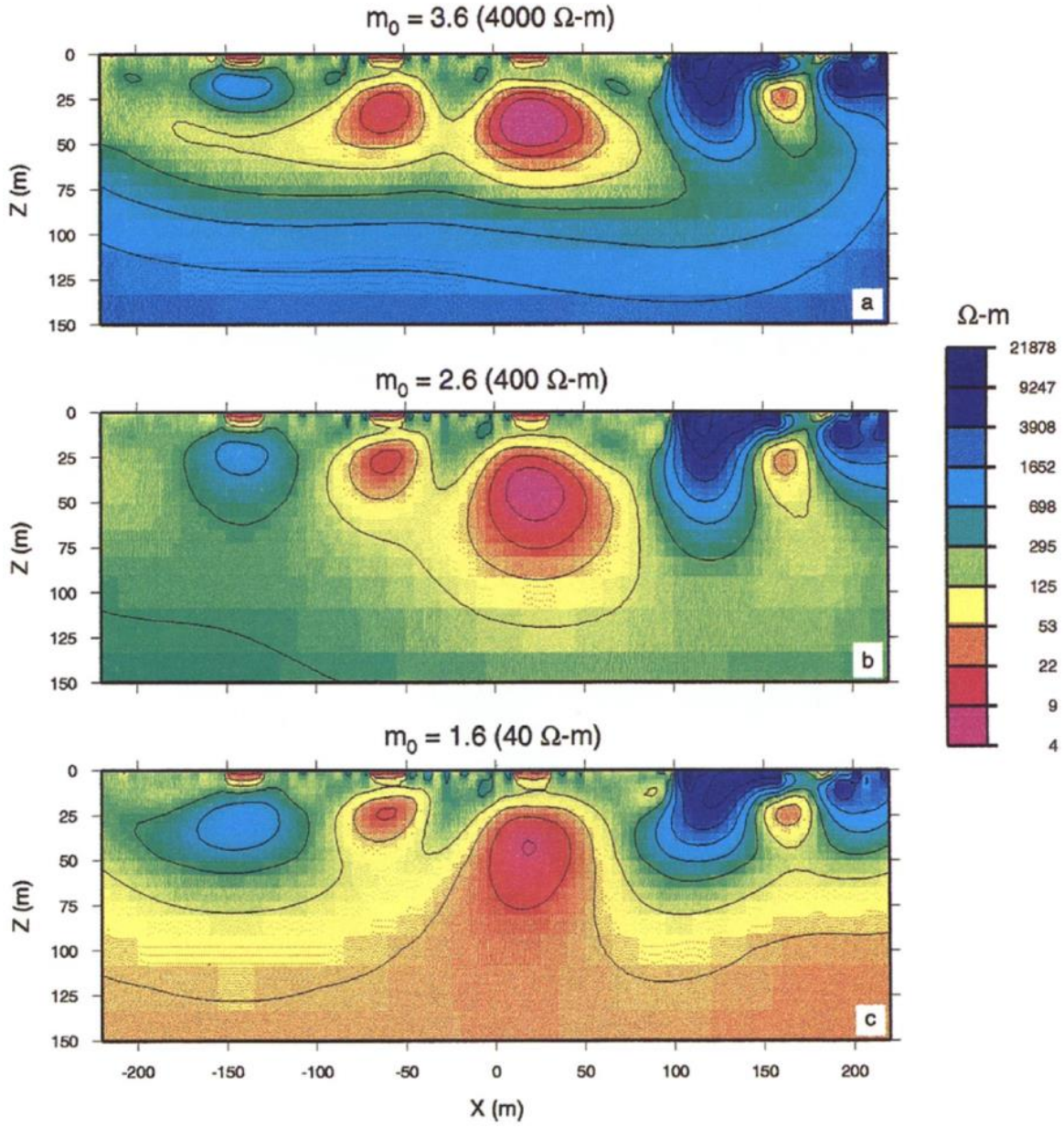


Figure 3. Example from/of Oldenburg-Li (1999) process for determining the DOI. Three inversion runs with very different reference model halfspaces (4000 ohm-m, 400 ohm-m, and 40 ohm-m) produce three models. Where the model results are similar, the inversion features are data-driven. Where the models vary, usually at depth, the

inversion features below the DOI depth are model-driven. The depth at which the data-driven features end is defined to be the DOI.

4.3 Model Space Analysis

Although not specifically a DOI investigation, another method useful in exploring the depth at which models are poorly constrained is to perform a model-space search for a distribution of probable models fitting a given data set. Having searched the model space exhaustively, equivalence problems and other model-space related issues can then be included in the DOI discussion. The obvious drawback of this approach is the massive computational cost to perform the model-space search, which can make performing this analysis on large datasets untenable. Furthermore, the result of such an analysis is a distribution of possible models and interpreting this into actual geologic results is not straightforward.

Note that the model space investigation approach is fundamentally concerned with resolution and model equivalence and is not primarily concerned with determination of DOI's, although certainly, at depth, models become spurious and extremely poorly constrained and a DOI can be inferred.

5.0 AEM Data Example

In this section we present examples of AEM data and their associated DOI's. We first examine the DOI's included in the exported Aarhus Workbench inversion results and how they, and additional DOI's selected from the same data set but using different thresholds, relate to the final inverted earth models. Next, available borehole information is added to the analysis to provide ground truth to the discussion. Finally, examples of the application of the approach presented by Oldenburg and Li (1999) are presented and discussed.

5.1 The GERDA Database

When data is first imported into the Aarhus Workbench a project database is created. The database follows the format of a GERDA database (GEUS, 2012). GERDA, short for "GEophysical Relational DAtabase", is the Danish national database on shallow geophysical data, established in 1998. All information on data acquisition, data processing and the inversion procedure can be stored, facilitating full reprocessing and inversion of data when needed.

In the Aarhus Workbench, all raw AEM data, processing performed, and inversion results are included in the project GERDA database from which cumulative sensitivities, as described by Christiansen and Auken (2012), can be derived. An example of one

sounding's listed sensitivities and the calculated cumulative sensitivities are plotted in Figure 4. The orange line plots the original sensitivities and the blue line the calculated cumulative sensitivities. Also indicated in Figure 4 are the locations of cumulative sensitivity thresholds 1.2 (square) and 0.6 (circle) which are what the Workbench automatically lists for each flight position in the exported Workbench inversion results xyz file. In the example shown, the upper DOI is at a depth around 210 m and the lower DOI is at an approximate depth of 263 m.

5.2 SCI Inversion Results

Example SCI inversion results for three SkyTEM AEM flight lines are presented in Figure 5. Blue colors are electrically conductive materials and red colors represent more resistive materials. The west to east line on top is approximately 270,000 ft long (about 51 miles or 82 km) and the center south to north line is approximately 390,000 ft long (about 74 miles or 119 km). The bottom profile also runs from south to north and is approximately 290,000 ft in length (about 55 miles or 88 km). The data gaps along the flight lines are due to masking of electromagnetic coupling effects. The flight-line distance and depth units are in feet in order to meet the client's needs.

In the top profile in Figure 5 (Line 100201), multiple sub-horizontal zones of conductive (deep blue colors) and resistive (yellow to red colors) units are shown. There is a conductor, approximately 200 ft thick (from elevation 1400 ft to 1200 ft), entering the profile from the west (left side) that thins out about a third of the way along the profile. Then a deeper conducive zone, about 100 ft to 150 ft thick between elevations 1200 ft to 1000 ft, with a slight upward tilt progresses across the profile to the east. Beneath the thin conductor on the eastern third of the profile, there is a thick resistive unit (40 ohm-m to 70 ohm-m), that is approximately 400 ft to 600 ft thick). Beneath this resistive unit there is some indication of another, more conductive, unit with resistivities in the range of 15 – 20 ohm-m.

Line 201001, the center south to north profile in Figure 5, exhibits similar geology and resistivities to Line 100201. On the south end of the profile (left side) is a topographic low, a valley, with resistive (>60 ohm-m) near-surface material. It appears that this valley had cut into the 200 ft thick, slightly north-dipping, conductive zone between elevations 1450 ft to 1200 ft, that is similar to that observed along Line 100201. While the deep, thick, very resistive unit observed on the east end of Line 100201 is not readily apparent on this profile, there are still indications of a 25-30 ohm-m unit between elevations 1000 ft to 500 ft that is somewhat irregular in its character that is overlying a 15-20 ohm-m unit similar to that observed on line 100201.

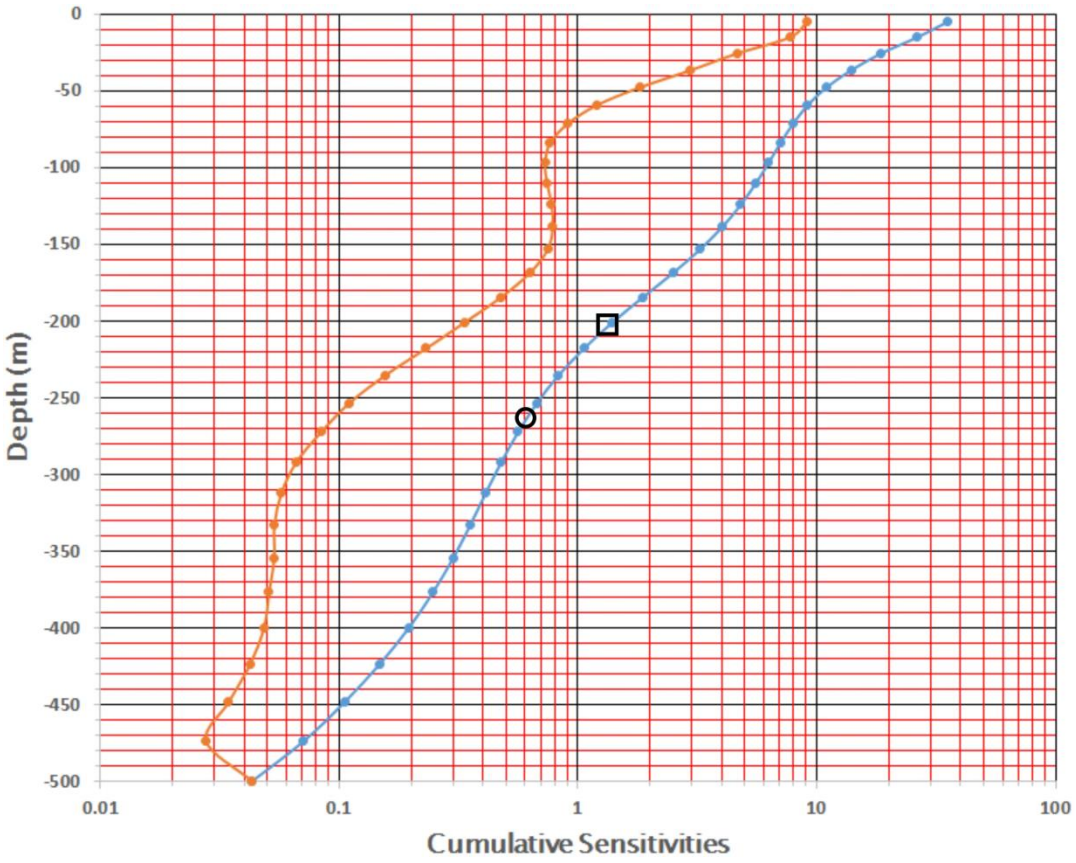


Figure 4. Example of exported sensitivities (orange line) from the GERDA database and the calculated cumulative sensitivities (blue line). Depths, in meters, are on the vertical axis. The horizontal axis is in dimensionless units of cumulative sensitivity. The black square is the location at which the cumulative sensitivity is 1.2 leading to a DOI of approximately 208 m depth. The black circle is the location at which the cumulative sensitivity is 0.6 leading to a DOI of approximately 263 m depth. DOI's for cumulative sensitivity thresholds 1.2 and 0.6 are included in the exported Workbench inversion results xyz file per the inversion configuration setup file.

The bottom profile in Figure 5, Line 202001, also exhibits similar geology to the other two profiles with the exception that the conductive zones are thinner and there are two well-defined resistive zones. One is approximately 250 ft to 400 ft thick between elevations 1200 ft and 800 ft with a resistivity range of 25 ohm-m to 50 ohm-m and the other is relatively continuous unit about 300-400 ft thick between elevations 550 ft and 150 ft with a similar resistivity range. Below this deeper resistive unit a more conductive zone (ranging from 10 ohm-m to 20 ohm-m) is present. It ranges in elevation from approximately 150 ft to the bottom of the profile at elevation -250 ft.

5.3 DOI Contours – Original Set

White lines representing the DOI contours for cumulative sensitivity thresholds 1.2 and 0.6, the global thresholds suggested by Christiansen and Auken (2012) and selected by default in the Aarhus Workbench, are presented in Figure 5. These are the "upper" and "lower" DOI's included in the exported inversion results file.

There are several observations that can be made about the profiles in Figure 5. The first, per the theory presented in Section 2 and the example shown in Figure 1, is that when the geology is more electrically conductive, the DOI is shallower and when the geology is more resistive, the DOI is deeper. An illustrative example of this is shown in the profile for Line 100201. On the western side of the line the lower DOI (0.6) is at an approximate elevation of 1100 ft. As one progresses eastwards and into the region where the subsurface becomes quite resistive, the 0.6 DOI drops down to an approximate elevation of 700-800 ft. This DOI behavior is an indication that the sensitivities are being calculated properly.

Next in Figure 5, in the same top profile (Line 100201), the 'lower' DOI (0.6) hovers just under the shallower conductive zone on the west side of the profile, transitions in the middle of the profile, and then clearly hovers just above the well-defined resistive zone on the eastern half of the profile. In the middle profile the 0.6 DOI is also located just under the shallow conductor except on the western side where it drops in elevation under the resistive zone located on the surface in the topographic valley area.

In the bottom profile in Figure 5 the lower DOI is situated between elevations 400 ft to about 800 ft within the somewhat discontinuous conductive zone except on the far northern end (right side) where it dips down into the resistive zone between elevations 500 ft to 400 ft. Clearly the lower DOI is above (except on the right side) the well-defined resistive zone between elevations 500 ft to -100 ft and the conductive zone deeper than elevation -100 ft.

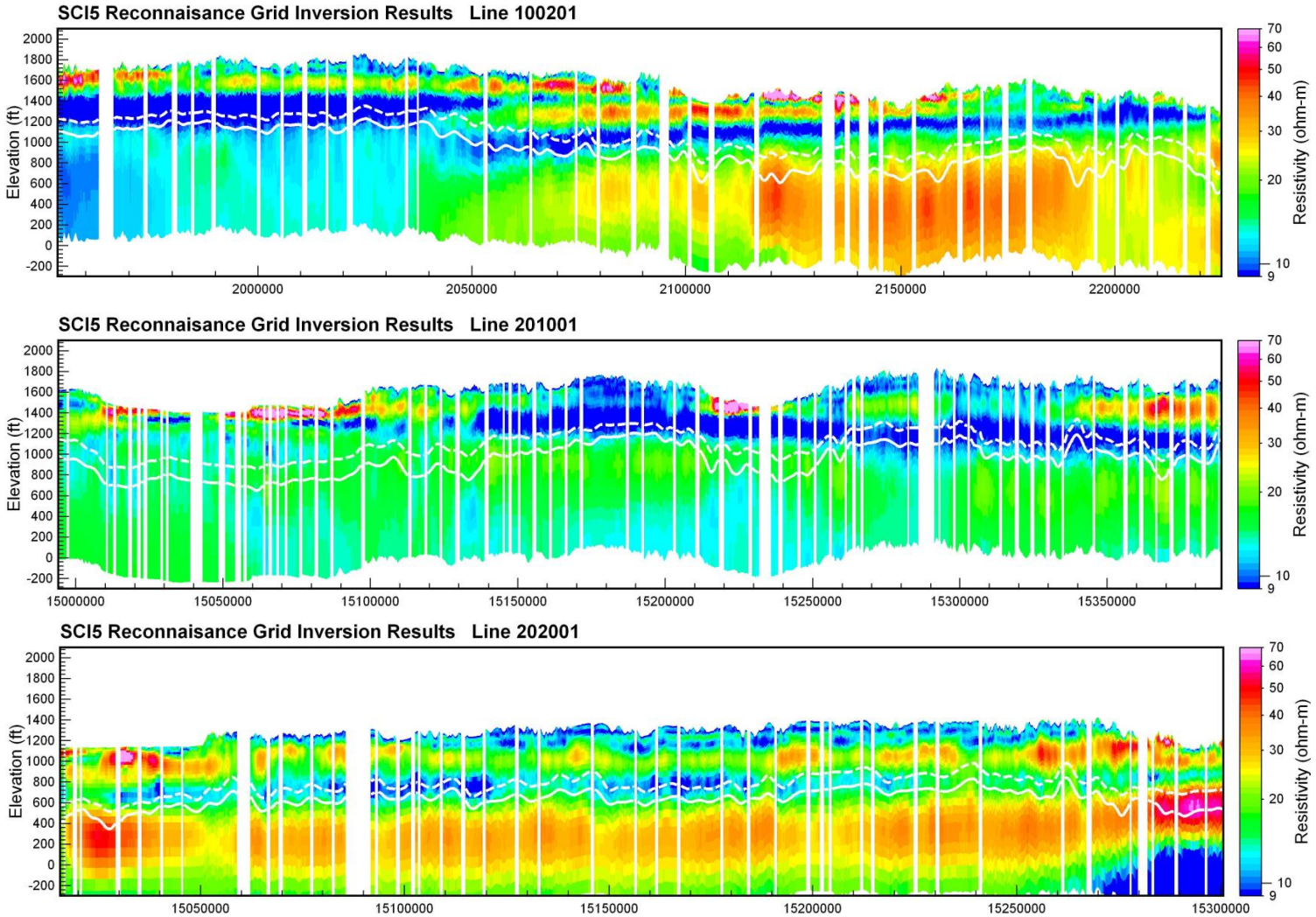


Figure 5. Aarhus Workbench SCI inversion results for west to east (top, left to right) and south to north (bottom & center, left to right) oriented flight lines. The data gaps are where electromagnetic coupling affects have been removed. The dashed lines represent the DOI at a cumulative sensitivity threshold of 1.2 and the solid lines the DOI at a cumulative sensitivity threshold of 0.6. Elevation and distance units are in feet.

This suggests that an examination of additional cumulative sensitivity threshold values leading to additional DOI values is necessary in order to determine a threshold that supports what is observed in the inverted profiles.

5.4 Comparison of the Theoretical DOI to the Workbench DOI's

In order to make a comparison, between the Workbench DOI's and theoretical DOIs based on equation (5), theoretical DOI's have been calculated for the example AEM data set and are displayed in Figure 6 along with the Workbench-default upper and lower DOI's. Spies (1989) indicates that typical TEM noise levels range from 0.2 to 0.5 nV/m^2 in winter and from 2 to 10 nV/m^2 in summer for voltage (dB/dt) measurements. A noise level of 0.5 nV/m^2 was used in the calculation for the DOI displayed in Figure 6.

First off, the theoretical DOI contours (the red lines in Figure 6) are obviously much lower in elevation (i.e. deeper) than either of the default DOI's. This is likely due to late time noise in the acquired AEM data (more noise than what is theoretically accounted for by using a noise level of 0.5 nV/m^2 in equation (5)).

Secondly, the theoretical DOI contour exhibits behavior that suggests it is very sensitive to the geology in the section. The theoretical contours drop lower when they are under resistive materials and move higher when they are under conductive material. For example, make an examination of the theoretical DOI contour in the center profile in Figure 6, Line 201001. Beginning on the south end of the line (left side), the theoretical DOI drops lower between tick marks 15010000 and 15090000 and 15215000 and 15230000 which is where the section in the near-surface is more resistive.

5.5 DOI Contours – Expanded Set

In Figure 7, in addition to the 1.2 and 0.6 cumulative sensitivity thresholds, three additional cumulative sensitivity values are marked with colored circles. The blue circle marks a cumulative sensitivity of 0.4, the green circle a cumulative sensitivity of 0.2, and the red circle the cumulative sensitivity of 0.1. In this example, the DOI for the 0.4 threshold is approximately -309 m depth. For the 0.2 threshold (green circle), the DOI is approximately -400 m depth. For the 0.1 threshold (red circle), the DOI is approximately -452 m depth.

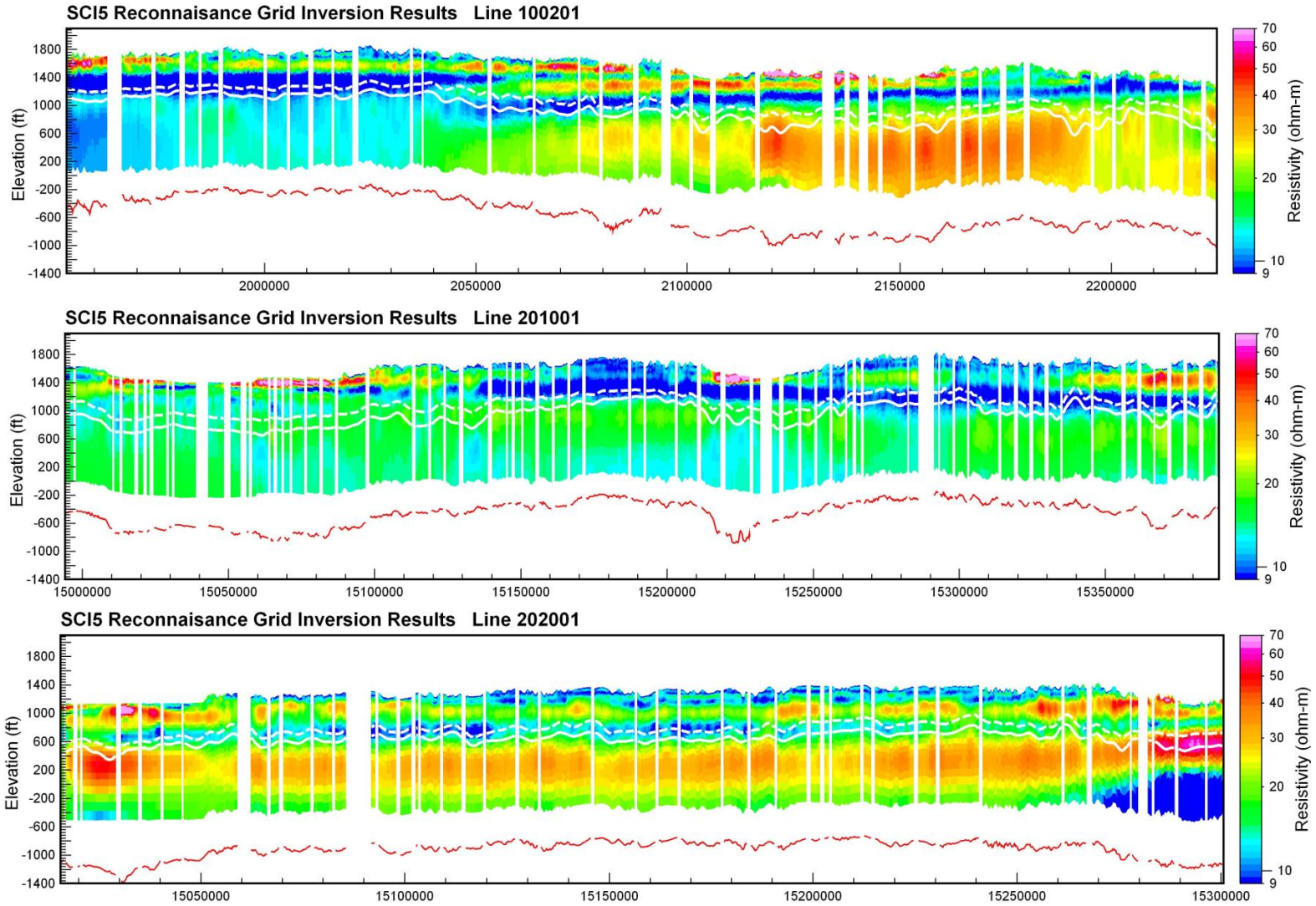


Figure 6. Aarhus Workbench SCI inversion results with the "default" upper and lower DOI's per Figure 5 plus the theoretical DOI (red line) based on equation (5) using a 0.5 nV/m^2 noise level. Elevation and distance units are in feet.

In Figure 8 the three example SCI inversion profiles are presented with DOI contour lines at cumulative sensitivity thresholds 1.2 (dashed white line), 0.6 (solid white line), 0.4 (green line), 0.2 (brown line), and 0.1 (black line). There is obviously a DOI depth progression as the cumulative sensitivity decreases. On the Line 100201 profile the 0.4 DOI contour is just 100 ft below the 0.6 DOI contour line. The 0.2 DOI contour line is about 400 ft deeper than the 0.6 DOI contour line and the 0.1 DOI contour line is about 500 ft to 800 ft below the 0.6 DOI contour line. Remember the variations are functions of the resistivity of the sounding for which the DOI is calculated.

On the center profile in Figure 8, Line 201001, the separation of the DOI contour lines for the different cumulative sensitivity thresholds varies from 100 ft (0.4) to 300 ft (0.2) to 600 ft (0.1) below the 0.6 DOI contour line underneath the resistive topographic valley on the west side of the profile to 75 ft (0.4) to 225 ft (0.2) to 425 ft (0.1) below the 0.6 DOI contour line in the center of the profile.

The DOI contours for the lower cumulative sensitivity thresholds are much deeper in the bottom profile in Figure 8 then the top and center profiles because of the two resistive zones, especially the deeper thick zone. The 0.1 DOI contour line (black) is generally following the base of the deep, thick resistive zone in the bottom profile to almost -250 ft elevation, and in some cases below that depth.

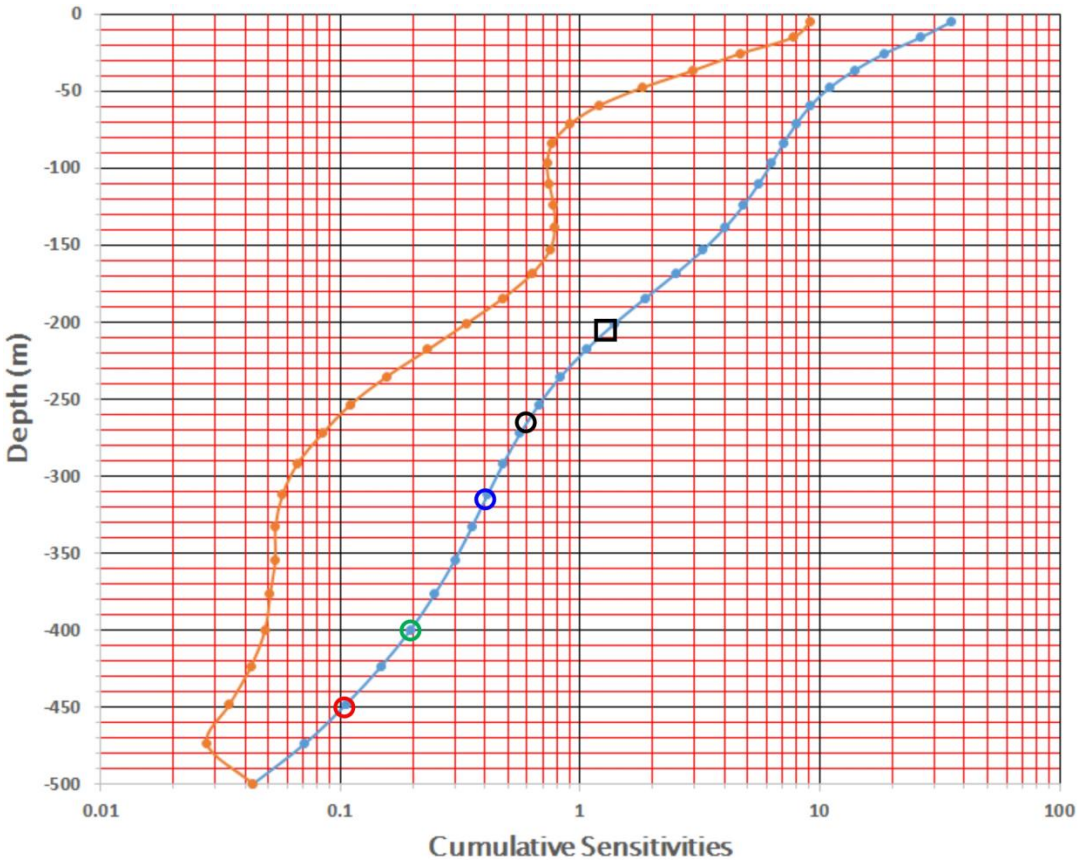


Figure 7. Example of exported sensitivities (orange line) from the GERDA database and the calculated cumulative sensitivities (blue line). Depths in meters are on the vertical axis. The horizontal axis is in units of cumulative sensitivity. The black square is the cumulative sensitivity at 1.2 (DOI ~ 208 m depth); The black circle is the cumulative sensitivity at 0.6 (DOI ~ 262 m depth); The blue circle is the cumulative sensitivity at 0.4 (DOI ~ 309 m depth); The green circle is the cumulative sensitivity at 0.2 (DOI ~ 400 m depth) The red circle is the cumulative sensitivity at 0.1 (DOI ~ 452 m depth).

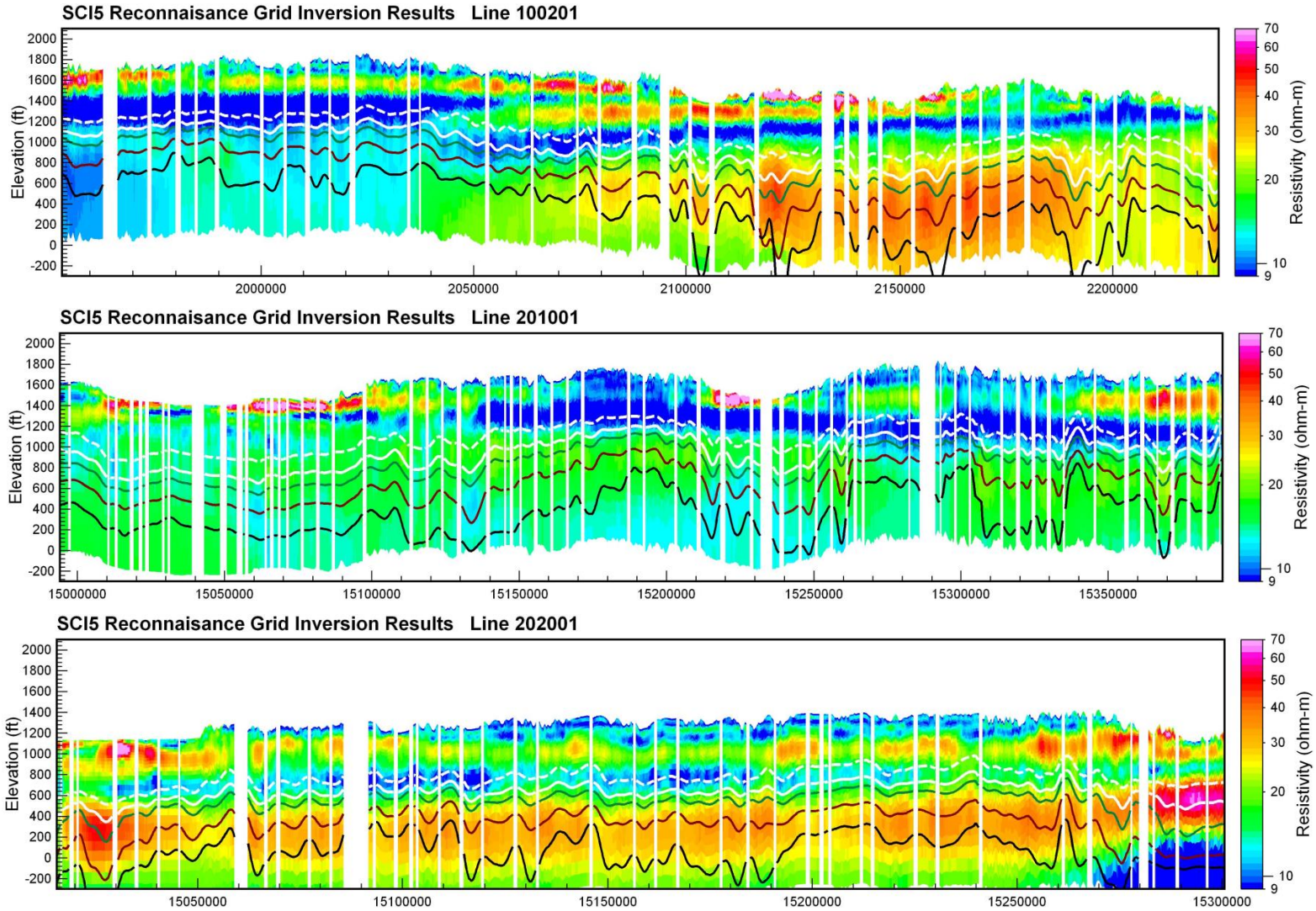


Figure 8. Aarhus Workbench SCI inversion results with DOI's based on cumulative sensitivity thresholds 1.2 (dashed white line), 0.6 (solid white line), 0.4 (green line), 0.2 (brown line), and 0.1 (black line). Elevation and distance units are in feet.

5.6 Ground Truth - DOI Contours and Boreholes

The obvious next question is whether the information indicated by a specific DOI contour is real or is just a feature of the regularization process of the inversion. To help assist in this determination, available borehole information is now added to the profiles. These are presented in Figure 9 along with the 0.6 and 0.1 DOI contours.

The borehole information presented in Figure 9 is derived from the University of Nebraska-Lincoln Conservation and Survey Division (CSD) test hole data set (CSD, 2014) and the Nebraska Oil and Gas Commission (NOGC, 2015).

As discussed before, the test holes are vital to the understanding of the subsurface conditions in a survey area and, in particular, for performing comparisons with the AEM inversion results (Schamper et al., 2014). CSD test holes that lay within 15,000 ft (2.84 miles or 4.573 km) of the flight lines and NOGC holes that lay within 60,000 ft (11.37 miles or 18.293 km) of the flight lines have been plotted on the profiles. The CSD holes, being water wells, have a limited depth extent, usually not more than 450 feet, and, though some were used as near-surface constraints in the inversions, they had minor impact, if any, on the DOI's at those locations. The deeper NGOC wells, being oil and gas wells, extend much deeper, far below the depth extent of the AEM sensitivity. The CSD borehole logs provide a good comparative base for the shallow AEM data and the NGOC borehole logs provide the critical key to evaluating features in the deeper AEM data and, in particular, what cumulative sensitivity threshold(s) should be used to determine realistic and data-based depths of investigation. Note that the NGOC boreholes were too far from the flight lines to be used as constraints in the inversions.

An examination of the shallower CSD borehole resistivity logs in the three example profiles in Figure 9 shows that general agreement between the borehole electric logs and the AEM data occurs across the project area, although small deviations occur in some locations, especially where wells could be too far off the flight lines. In the center of the top profile, Line 100201, CSD boreholes 14-A-53, 15-A-53, 10-B-53, and 41-A-52 all indicate a thin resistive zone (30-70 ohm-m) at the exact same depths as indicated by the AEM data, around an elevation between 1500 ft and 1600 ft. In addition, CSD boreholes 41-A-52, 40-A-52, and 09-LC-13 actually indicate two resistors at the tops and bottoms of their logs at an elevation of about 1300 ft. The second deeper resistor also matches the thin resistor indicated in the AEM data in the middle of the profile between elevations 1200 ft to 1400 ft.

The shallow CSD boreholes shown in the bottom profile in Figure 9, Line 202001, similarly match the AEM data. On the south end of the profile (left side), CSD borehole

21-A-62 shows a resistor (>60 ohm-m) at the exact same depth, elevation, and thickness as the AEM data. CSD borehole 4-B-63 is only deep enough to match the very near surface conductive material indicated by the AEM data. However, CSD boreholes 9-B-63, 11-B-63, 6-A-63, 7-A-63, and 13-B-63 all indicate both the shallow conductor observed in borehole 4-B-63 and the AEM data but also the slightly deeper resistive material that extends across the profile between elevations 950 ft to 1150 ft.

On Line 201001, the middle profile in Figure 9, three deep NGOC boreholes are displayed. Borehole logging in these holes began at depths of 200 ft to nearly 300 ft below the ground level and continued well below the depth of the AEM profile.

In the middle of the profile are the logs for boreholes 26167210030000 (left) and 26167190000000 (right). These test holes are located about 10,000 ft to 20,000 ft from the flight line and so, as mentioned above, were not used as constraints in the inversions. A third deep borehole, 26143190000000, is on the southern end of the line (left side), but is about 40,000 ft off the flight line. Examination of these logs indicates that there appear to be four distinct resistivity zones: 1) Elevations 1400 ft to 1160 ft – conductive (<10 ohm-m); 2) Elevations 1160 ft to 520 ft – resistive (25-40 ohm-m); 3) Elevations 520 ft to 280 ft – conductive (<10 ohm-m); and 4) Elevations 280 ft to below the depth of the profile view – resistive (>60 ohm-m).

Comparison of these borehole resistivity zones with the AEM inversion model profile indicates very good visual agreement, even given the offset distances of the boreholes from the flight line. This implies that the sensitivity of the AEM data to the subsurface is very much deeper than the default “lower” DOI, cumulative sensitivity threshold 0.6. The agreement indicates that the actual depth of investigation threshold, from a detection/mapping perspective, is in the vicinity of the 0.1 cumulative sensitivity threshold displayed in the profile.

Equation (4) can also be used to calculate DOI’s equivalent to the cumulative sensitivity-based DOI’s developed per the Christiansen-Auken method. By using slowly increasing noise levels in equation (4), an iterative process resulted in the two theoretical DOI’s (brown and red lines) that are displayed in Figure 10. These DOI’s were calculated using noise levels of 4 nV/m^2 and 150 nV/m^2. The upper brown line nearly overlays the 0.6 cumulative sensitivity DOI and the lower red line DOI approximates the 0.1 cumulative sensitivity DOI. While the 150 nV/m^2 noise level is extremely far above the noise level ranges suggested by Spies (1989) of 0.2 to 0.5 nV/m^2 in winter and from 2 to 10 nV/m^2 in summer for voltage (dB/dt) measurements, the lower theoretical DOI in Figure 10 using 4 nV/m^2 is a quite reasonable noise level

value being in the low summer range. Note that the example AEM data set discussed in this paper was acquired in early October.

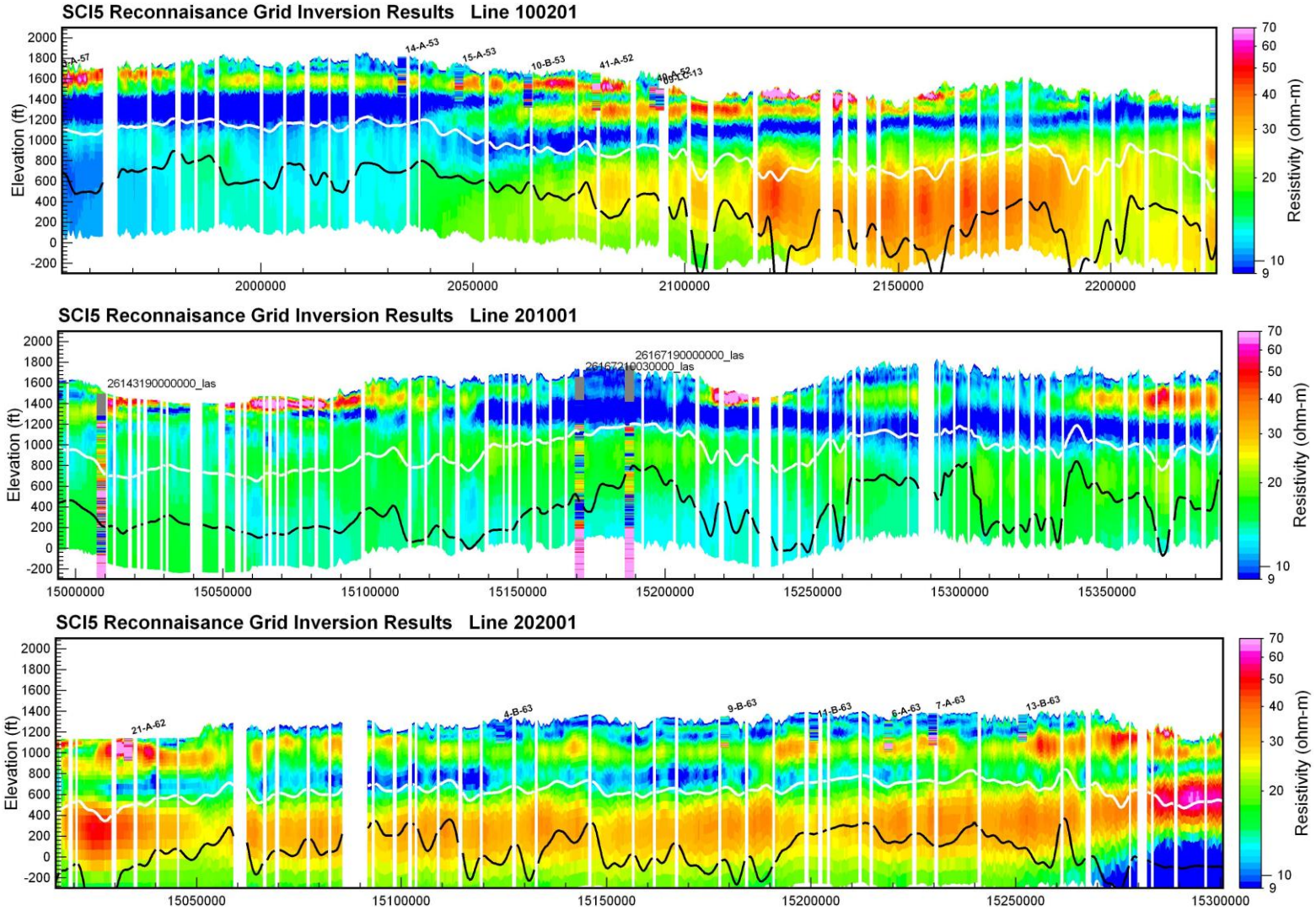


Figure 9. Aarhus Workbench SCI inversion results with DOI's based on cumulative sensitivity thresholds 0.6 (solid white line) and 0.1 (black line) and available borehole resistivity logs from the Nebraska CSD (2014) and the NOGC (2015). Elevation and distance units are in feet.

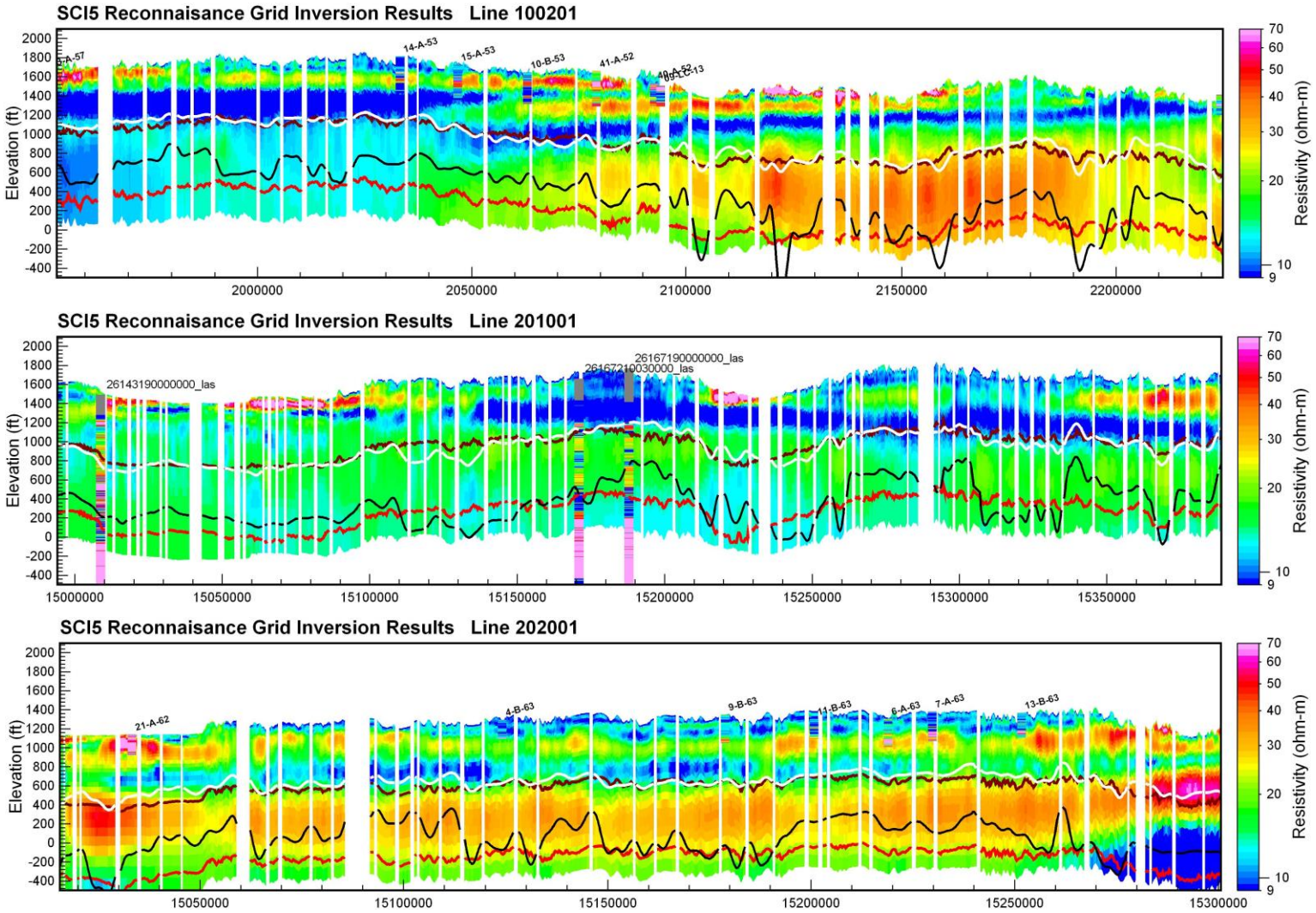


Figure 10. SCI inversion results with DOI's based on cumulative sensitivity thresholds 0.6 (solid white line) and 0.1 (black line), borehole resistivity logs, and theoretical DOIs based on equation (4) using noise levels of 4.0 nV/m^2 (red line) and 150 nV/m^2 (brown line). Elevation and distance units are in feet.

5.7 Oldenburg-Li Method For Determination of the DOI

As discussed above in Section 4.2, the Oldenburg-Li approach to determining an approximate DOI is to run multiple inversions with different reference halfspace models. The inversion results are considered to be data-driven when they present similar information and are considered model-driven (i.e. inversion regularization effects) when the results are considerably divergent, especially at depth.

An application of the Oldenburg-Li approach to the example AEM data under discussion is presented in Figure 11. We note a deviation from Oldenburg-Li and use starting models rather than reference models, as Aarhus workbench does not support reference models. The inversion results are quite sensitive to the starting model, making this approach a reasonable alternative. The center profile is the same as the bottom profile in Figure 9 which had a starting halfspace of 10 ohm-m. The top profile had a starting halfspace model of 40 ohm-m and the bottom profile had a starting halfspace of 3 ohm-m.

When examining the results in Figure 11 it is important to keep in mind the average residual data errors for each inversion run. This is one of the caveats of the Oldenburg-Li approach; namely, that the final inversion data errors must be similar in order to compare inversion results. The L2 norm of the residual data error (Resdata) for the 10 ohm-m starting halfspace inversion result is 0.539 which is about average for a SkyTEM data set (usually 0.45 to 0.55). The average Resdata for the 40 ohm-m starting halfspace inversion result was 0.547 and for the 3 ohm-m starting halfspace it was 0.799. This indicates that since the Aarhus inversion residuals are dependent upon the starting model, the inversion may be prone to getting caught in local minima.

Obviously, the 3 ohm-m starting halfspace inversion model (bottom profile, Figure 11) is much different (<10 ohm-m below an elevation of 950 ft) than either the 10 ohm-m or 40 ohm-m starting halfspace inversion results which is in line with a very high Resdata value (0.799). The 3 ohm-m starting halfspace can be observed at the bottom of the profile. The 3 ohm-m inversion result cannot be compared with the other inversion models to determine what is data-driven and what is model-driven. In the case of a blind inversion when a reasonable starting model cannot be assumed, results can suffer. However, this is a nice side effect of the Oldenburg-Li approach. That is, while performing this analysis, the nature and behavior of the inversion is captured and investigated.

However, the 10 ohm-m and 40 ohm-m starting halfspace inversion results are quite similar, except at elevations lower than 200 ft, which is in line with their Resdata average error values (0.539 and 0.547, respectively).

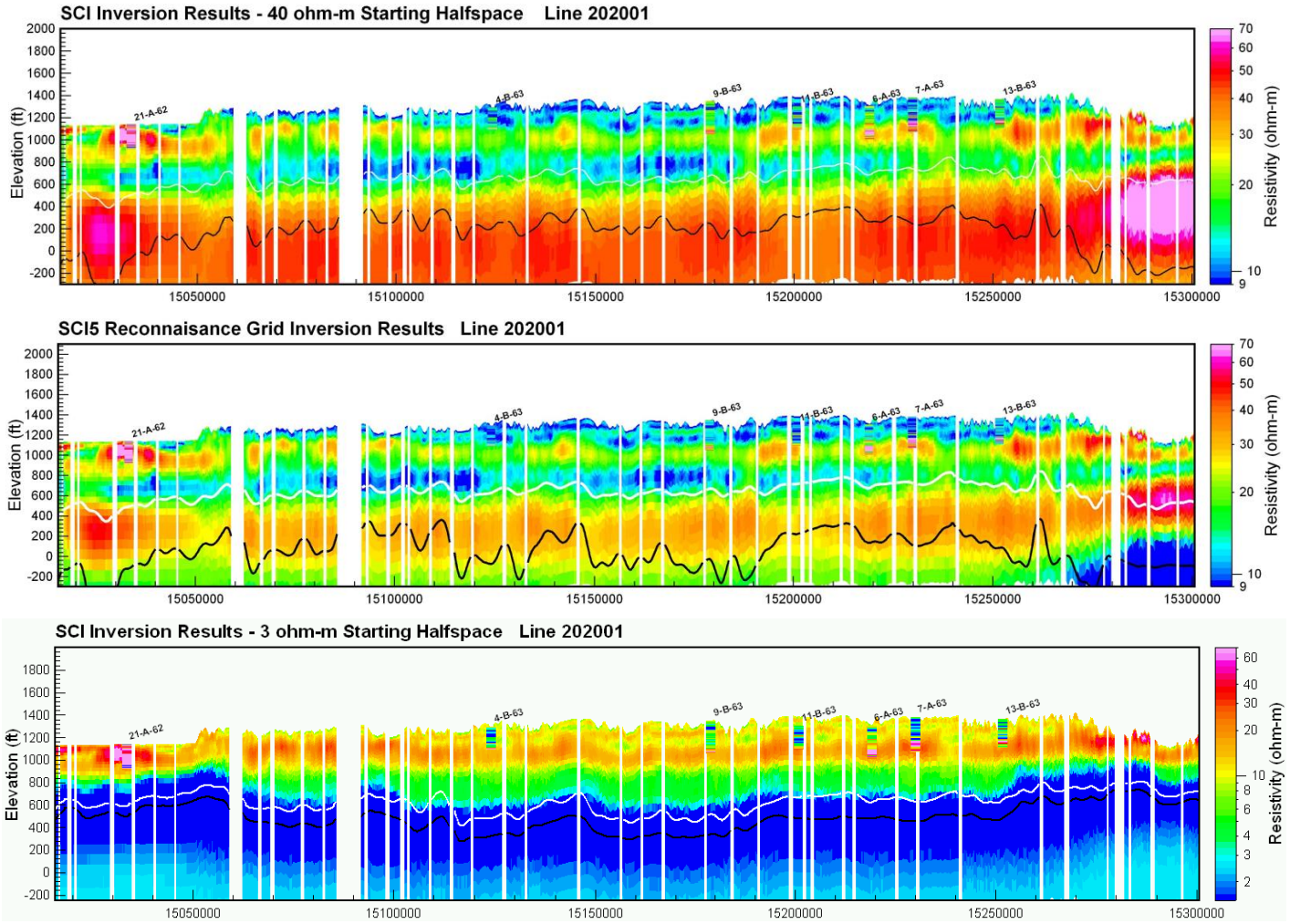


Figure 11. Aarhus Workbench SCI inversion results with DOI's based on cumulative sensitivity thresholds 0.6 (solid white line) and 0.1 (black line) and available borehole resistivity logs from the Nebraska CSD (2014). Top – 40 ohm-m starting halfspace with average Resdata Error = 0.547. Middle – 10 ohm-m starting halfspace (same as in previous figures) with average Resdata Error = 0.539. Bottom – 3 ohm-m starting halfspace with average Resdata Error = 0.799. Elevation and distance units are in feet. The resistivity range is 9–70 ohm-m for all three profiles.

The resistivity distributions in each profile are in good agreement as are the DOI contours for cumulative sensitivity threshold 0.6 (solid white lines).

The resistivities at depth (<400 ft elevation) in the 40 ohm-m starting model profile are in the range of 30-60 ohm-m whereas the resistivities at depth in the 10 ohm-m starting halfspace are in a slightly more conductive range, 25-50 ohm-m. The cumulative sensitivity threshold 0.1 DOI's are slight different for each of these models. The 40 ohm-m halfspace 0.1 DOI is slightly higher in elevation across the profile (around +200 ft to +300 ft) across the profile than the 10 ohm-m halfspace 0.1 DOI (around 0 ft to -150 ft elevation). Otherwise they match quite well.

The next step is to quantitatively examine the differences between the two models.

In the Oldenburg-Li (1999) process, the next step after running the three inversions is to represent the actual differences between the models by calculating what they call the "DOI Index, R" per the following relation:

$$R(x,z) = \frac{m_1(x,z) - m_2(x,z)}{m_{1r} - m_{2r}} \qquad (10)$$

where m_{1r} and m_{2r} are the reference (in our case starting) models (40 ohm-m and 10 ohm-m in this case) and m_1 and m_2 are the recovered inversion models. Oldenburg and Li characterize R as approaching zero where the two inversions produce the same result regardless of the value of the reference models and as approaching unity at locations where the inversion results match the reference model value. Those data value areas that approach zero are assigned high credibility and those that approach unity are assigned low credibility.

The Oldenburg-Li DOI Index plot for the 10 ohm-m and 40 ohm-m starting halfspace models in Figure 11 is presented as the bottom plot in Figure 12 along with the two reference halfspace inversion models. While Oldenburg and Li indicate that the range of R should be between 0 and 1, the actual range for the calculated DOI Index data presented in Figure 12 is from -0.53 to 1.98 due to the narrow band of starting models that was necessary in our study. Blue colors represent areas where the models match (low DOI Index values), and red colors areas where they don't match (high DOI Index values).

The DOI's based on the cumulative sensitivities 0.6 and 0.1 are also overlain on the plots in Figure 12. Note that the 0.6 DOI, the Christiansen-Auken "lower" DOI, plots well within the blue area, that is, where the models match, meaning that this DOI is set shallower in depth than where the inversion results are still data driven.

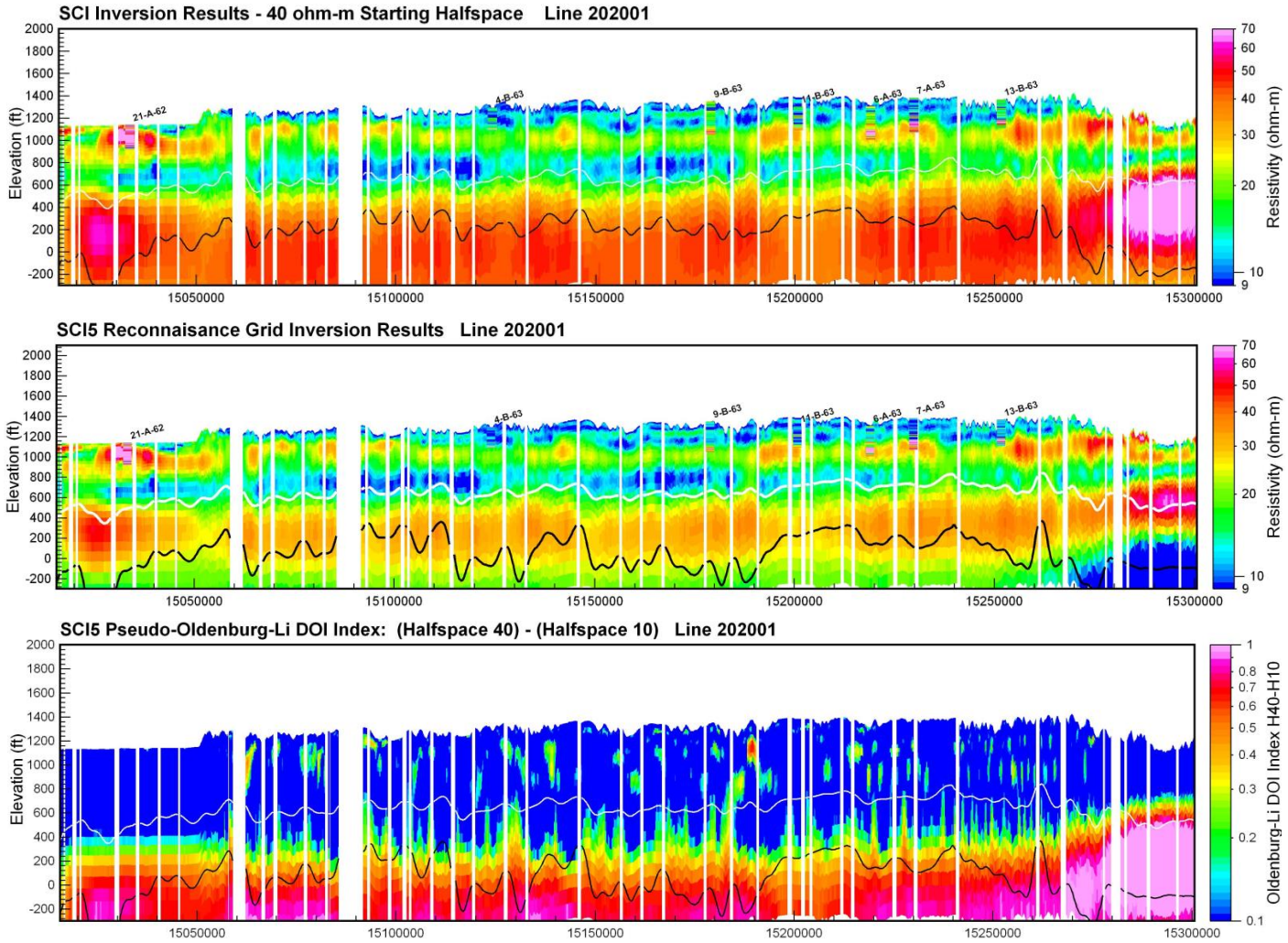


Figure 12. Aarhus Workbench SCI inversion results with DOI's for cumulative sensitivity thresholds 0.6 (solid white line) and 0.1 (black line) and available borehole resistivity logs. Top – 40 ohm-m starting halfspace. Middle – 10 ohm-m starting halfspace. Bottom – Calculated Oldenburg-Li DOI Index (Note that the range is not completely $0<x<1$). Elevation and distance units are in feet.

The 0.1 DOI, however, generally lies in the yellow to orange colored zones (representing DOI Indices of 0.2 to 0.4) just above the red colored areas, which are the low credibility results, in the figure.

So one would conclude that the DOI for this data is probably just above the cumulative sensitivity 0.1 DOI for the 10 ohm-m halfspace starting model result since the residual data errors are slightly smaller than for the 40 ohm-m starting halfspace model.

6. Discussion and Conclusions

In their paper Christiansen and Auken (2012) sum up the value of the DOI as follows: "*A calculation of the DOI is crucial when building geologic or hydrological models from EM data as the validity of the models varies strongly with data noise and the resistivity of the layers themselves. Without the DOI estimate, it is next to impossible to judge when the information in the model is driven by the data or is just an effect of the starting model or the regularization of the inversion.*"

Subscribing to this philosophy, this paper has presented both the theoretical basis for estimation of the DOI per Nabighian and Macnae (1989) and Spies (1989) and the practical application for determination of the DOI using the model to data sensitivities inherent to the Jacobian matrix (Christiansen and Auken, 2012) and inversion using multiple starting models (Oldenburg and Li, 1999).

The inversion results from many AEM data sets that have been processed and inverted through the Aarhus Workbench strongly suggest that the default DOI's exported with the Workbench inversion results, namely those DOI's based on cumulative sensitivity thresholds 1.2 and 0.6, are overly conservative (i.e. shallow) for many applications and do not fully encompass all the information presented in the inversion models. This is supported via the analysis of the Jacobian matrix and independently via multiple starting models with very different halfspace resistivities. DOIs, developed from global cumulative sensitivity thresholds 0.4, 0.2, and 0.1 and plotted on top of inversion results profiles allows for better discrimination between data-driven results and model-driven/inversion regularization results. Calculation of the Oldenburg-Li DOI Index and theoretical DOI's based on reasonable ambient noise levels serve to quantify the analysis. It is clear that, while variable, the global cumulative sensitivity threshold that should be used to determine appropriate DOI's for interpretation of AEM data is much closer to 0.1 than it is to 0.6, the default Workbench 'lower' DOI threshold.

Note that the word "*interpretation*" in the last sentence is of critical importance. For interpretive mapping, it is definitely feasible to interpret much deeper than the default DOI's. However, for something like Archie's Law, in which an exact formation resistivity

must be input in order to derive a pore fluid resistivity, using interpretative resistivity ranges may not be accurate or precise enough. It will depend on what the goal of the DOI analysis is, what the interpreter is trying to do, and how good is good enough in the derived solutions.

This paper has primarily been focused on the depth to which the electrical resistivity of the subsurface is well constrained. However, remember that there is a difference between *resolution* of a property and *detection* of a property. Resolution means that the properties of interest are accurately represented. Detection relates the fact that while the true value of a property may not be accurately resolved, there is still some sensitivity, in the data, to changes in that property and that is what is observed in the inversion result. The analysis presented in this paper has made the case that the DOI should be considered as a possible line of demarcation between resolution and detection.

Now the discussion presented here did not dwell on equivalent models that might fit the observed data equally well as compared to the base reference model (here the result using the 10 ohm-m starting halfspace). It was assumed that the model coming out of the Aarhus Workbench inversion process with the lowest residual data error was the best model. A thorough investigation of equivalency can only be addressed through application of a model space-type analysis. While the method presented by Oldenburg and Li (1999) does address the issue of equivalency to some degree, because the multiple alternative inversions suggest how much the inversion process can be moved in a given direction without violating the data, DOI comparisons and determinations cannot be made for data sets that cannot be fitted within the assigned data error (as in the case of the 3 ohm-m starting halfspace).

Finally, note that the formulation used by Christiansen and Auken (2012) does not incorporate sensitivity to equivalent models. The Oldenburg-Li (1999) approach can be thought of as a minimal model-space investigation and the full model-space investigation as an end-point of that approach.

7. References

Aarhus Geophysics, 2013. Aarhus Workbench, version 4.1.1.768, http://www.aarhusgeo.com/content/software/workbench/aarhus-workbench.html

Carney, C.P., Pierce, K.S., Abraham, J.D., Steele, G.V., Genco, A.G., Woolf, R.E.V., Cannia, J.C., and T. Meglich. 2014. Hydrogeologic Assessment and Framework Development of the Aquifers beneath the Brainard-Valparaiso Area of the Lower Platte South Natural Resources District in Eastern Nebraska. XRI Geophysics project findings report prepared for the Lower Platte South Natural Resources District, Lincoln, Nebraska.

Christiansen A.V. and Auken E. 2012. A global measure for depth of investigation. Geophysics, **77** (4), WB171-WB177.

CSD, 2014, University of Nebraska-Lincoln Conservation Survey Division Online Statewide Test Hole Database. Accessed multiple events in 2013-2014. Accessible at: http://snr.unl.edu/data/geologysoils/NebraskaTestHole/NebraskaTestHoleIntro.asp.

FlameRobin, 2014, http://www.flamerobin.org/

Geosoft, 2014. Oasis montaj version 8.1, Geosoft Incoporated, http://www.geosoft.com/support/downloads/updates/oasis-montaj

GEUS, 2012, Geological Survey of Denmark and Greenland GERDA database, http://www.geus.dk/gerda/gerda-uk.htm

Nabighian, M. N.. and Macnae, J. C., 1989. Time-domain electromagnetic prospecting methods. *in* Nabighian, M. N.. Ed.. Electromagnetic methods in applied geophysics. 2: Soc. Expl. Geophys.

NOGC, 2015, Nebraska Oil and Gas Conservation Commission. Accessible at: http://www.nogcc.ne.gov/olNOGCCOnlineGIS/

Oldenburg, D. W., and Y. Li, 1999, Estimating depth of investigation in DC resistivity and IP surveys: Geophysics, **64**, 403-416, doi: 10.1190/1.1444545.

Profile Analyst, Pitney Bowes Software. 2012. Encom Profile Analyst (PA), Version 12.0, Release Build 0, http://www.pbencom.com/products/Geophysics/encom-pa.shtml

Schamper, C., Jorgensen, F., Auken, E., and Flemming, E., 2014, Case history – Assessment of near-surface mapping capabilities by airborne transient electromagnetic data – an extensive comparison to conventional borehole data: Geophysics, **79** (4), B187-B199.

Spies, B. R., 1989, Depth of investigation in electromagnetic sounding methods: Geophysics, 54 (7), p. 872-888.